This document is downloaded from DR-NTU (https://dr.ntu.edu.sg)
Nanyang Technological University, Singapore.

Effect of Ni–P thickness on solid-state interfacial reactions between Sn–3.5Ag solder and electroless Ni–P metallization on Cu substrate

Kumar, Aditya; Chen, Zhong; Mhaisalkar, Subodh Gautam; Wong, Chee Cheong; Teo, Poi Siong; Kripesh, Vaidhyanathan

2005

Kumar, A., Chen, Z., Mhaisalkar, S. G. , Wong, C. C., Teo, P. S., & Kripesh, V. (2005). Effect of Ni–P thickness on solid-state interfacial reactions between Sn–3.5Ag solder and electroless Ni–P metallization on Cu substrate. Thin Solid Films, 504(1-2), 410-415.

https://hdl.handle.net/10356/95233

https://doi.org/10.1016/j.tsf.2005.09.059

© 2005 Elsevier B.V. This is the author created version of a work that has been peer reviewed and accepted for publication by Thin Solid Films, Elsevier B.V. It incorporates referee’s comments but changes resulting from the publishing process, such as copyediting, structural formatting, may not be reflected in this document. The published version is available at: [http://dx.doi.org/10.1016/j.tsf.2005.09.059].

Downloaded on 04 Apr 2024 15:03:21 SGT

Effect of Ni–P thickness on solid-state interfacial reactions between Sn–3.5Ag solder and electroless Ni–P metallization on Cu substrate

Aditya Kumar [a,*], Zhong Chen [a], S.G. Mhaisalkar [a], C.C. Wong [a], Poi Siong Teo [b], Vaidhyanathan Kripesh [b]

[a] School of Materials Science and Engineering, Nanyang Technological University, Nanyang Avenue, Singapore 639798, Singapore

[b] Institute of Microelectronics, 11 Science Park Road, Singapore 117685, Singapore

[*] Corresponding author. Tel.: +65 6790 4571; fax: +65 6790 9081.

E-mail address: aditya@pmail.ntu.edu.sg (A. Kumar).

Abstract

Solid-state interfacial reactions between Sn–3.5Ag solder and electroless Ni–P metallization on Cu substrate were investigated for three different Ni–P thicknesses. It was found that during interfacial reactions, Ni_3Sn_4 intermetallic grows at the Sn–3.5Ag/Ni–P interface along with the crystallization of electroless Ni–P layer into Ni_3P compound. Additional interfacial compounds (IFCs) such as Ni–Sn–P, Cu_3Sn, Cu_6Sn_5, $(Ni_{1-x}Cu_x)_3Sn_4$, and $(Ni_{1-x}Cu_x)_6Sn_5$ were also found to grow at the Sn–3.5Ag/Ni–P/Cu interfaces depending upon the Ni--P thickness. In the sample with thin Ni–P layer, formation of these IFCs appeared at lower aging temperature and within shorter aging duration than in the samples with thicker Ni–P. The complete dissolution of electroless Ni–P layer into Ni_3P and Ni–Sn–P layers was found to be the main cause for the growth of additional IFCs. Across the Ni_3P and Ni–Sn–P layers, diffusion of Cu and Sn takes place resulting in the formation of Cu–Sn and Ni–Cu–Sn intermetallics. It is shown in

this paper that multi-layered IFC growth at the Sn–3.5Ag/Ni–P/Cu interfaces can be avoided by the selection of proper Ni–P thickness.

Keywords: Electroless nickel; Solder; Interfacial reaction; Intermetallic compound

1. Introduction

Under bump metallization (UBM) is a combination of thin metallic layers which not only provides good solderable surface but also protects the underlying IC metallization from reacting with solder. During soldering process, UBM reacts with solder and forms a thin layer of interfacial compound (IFC). Formation of the thin layer is desirable to achieve good metallurgical bond. However, excess growth of the IFC affects the mechanical reliability of the solder joint which is a generic reliability problem in flip-chip solder joints [1–3].

Cu is a promising UBM material for Sn–Pb solder because of its good wettability with solder. However, Cu reacts rapidly with Sn of the solder forming thick layers of Cu–Sn intermetallics. This IFC over-growth problem is exacerbated in the case of Pb-free solders, used due to the legislation and environmental concerns, as the Pb-free solders are Sn-rich alloys constituting one or two more elements such as Ag, Cu, and Bi. The IFC growth has been found to be reduced in the case of Ni UBM, as the reaction between Ni and Sn is much slower than between Cu and Sn [4]. The Ni UBM can be deposited by various chemical and physical deposition techniques. Among them, electroless nickel with a thin layer of immersion gold has been considered as a promising UBM due to its easy processing and low cost.

Electroless nickel is a Ni–P alloy, where P comes from hypophosphite-reducing agent during the reduction of Ni from an ionic Ni solution. The presence of P in the electroless Ni–P UBM causes its complicated interfacial reactions with solder. The interfacial reactions include formation of Ni_3Sn_4 intermetallic and Ni_3P compound at the solder/Ni–P interface [2–12]. Other reaction products such as Ni_3Sn_2 and $Ni_{12}P_5$ were also reported [5,7], although Ni_3Sn_4 and Ni_3P were the major phases. Further, a ternary Ni–Sn–P

compound was also reported to form at the solder/Ni–P interface [8], which grew during liquid-state aging [9,10]. Recently, it was found [12] that this Ni–Sn–P compound can grow even during solid-state aging. Although numerous studies have been done on the interfacial reactions between solder and electroless Ni–P UBM, the understanding made so far on the influence of Ni–P UBM thickness on the interfacial reactions is incomplete. Accordingly, in this work, solid-state interfacial reactions between solder and electroless Ni–P UBM on Cu substrate were studied for different thicknesses of Ni–P UBM.

2. Experimental procedure

Cu (99.99%) plate of size of 70 mm × 25 mm × 6 mm was used to fabricate the multi-layered reaction samples Cu/Ni–P/ Sn–3.5Ag/Ni–P/Cu. The Cu plate was surface cleaned, first by polishing down to 1 μm finish, then by ultrasonically cleaning with acetone for 10 min, then by etching with 20 vol.% HNO_3 solution for a few seconds, and finally by cleaning with deionized water. Electroless Ni–P was plated on the surface cleaned Cu plate in two steps. In the first step, Cu surface was activated using the ruthenium-based commercial pre-initiator. Then, electroless Ni–P was plated on the activated Cu surface using commercial electroless nickel solution. Electroless Ni–P metallization, of three different thicknesses, was plated on the Cu plate by selecting the three different deposition times but at the same process conditions. Thin layer (~500 Å) of non-cyanide immersion gold was also deposited on the electroless Ni–P surface to protect the surface from oxidation.

The electroless Ni–P coated Cu plate was cut into two pieces of size of 40 mm × 25 mm × 6 mm and 30 mm × 25 mm × 6 mm, and then joined with each other using Sn–3.5Ag solder. Fig. 1 illustrates the set-up used to join the plates. The joint was formed during the reflow process by placing a number of small pieces of solder wires on the small electroless Ni–P coated Cu plate and pressing them by the big plate. No-clean paste flux was applied on both the plates before placing the Sn–3.5Ag wires. The reflow process was carried out in IR reflow oven (ESSEMTEC RO-06E) which involved preheating at 150 °C for 100 sec, then reflowing at 250 °C for 60 sec, and finally cooling down to 160 °C in the oven. Alumina spacers of thickness of around 650 μm were used to

maintain the uniform thickness of solder in between the plates. The joined plates were cut into a number of small samples with the help of diamond saw. Fig. 2 shows the schematic diagram of reaction sample.

As-prepared reaction samples were isothermally aged in the oven (Lenton WHT4/30) at 160, 180, and 200 °C for 48, 100, 225, and 400 h. After aging, the samples were removed from the oven and cooled in air to room temperature. JEOL JSM6360A scanning electron microscope (SEM) was used for microstructure analysis. For the cross-sectional SEM, the samples were cold mounted in epoxy and polished down to 1 μm finish. After polishing, solder etching was carried out to reveal the microstructure. Etching was done with 4 vol.% hydrochloric acid for a few seconds. Energy dispersive X-ray (EDX) spectroscopy was performed in the SEM to analyze the chemical composition of IFCs.

3. Results

The thicknesses of three as-plated electroless Ni–P layers were measured to be around 3.9, 7.3, and 9.9 μm while the P content was found to be around 16 at.%. According to their thicknesses, the electroless Ni–P layers are termed as thin, medium, and thick Ni–P.

3.1. As-prepared reaction samples

Fig. 3 shows the IFCs formed at the Sn–3.5Ag/Ni–P interface in the as-prepared samples having electroless Ni–P layers of different thicknesses. Regardless of Ni–P thickness, all the samples have similar interfacial microstructure and chemistry. Needle-type and chunky-type Ni_3Sn_4 intermetallic formed at the Sn–3.5Ag/Ni–P interface during the reflow, some of which spalled off into the molten solder. Underneath the Ni_3Sn_4, Ni–Sn–P layer formed whose composition was difficult to measure by EDX in the SEM owing to its submicron thickness. Underneath the Ni–Sn–P layer, a dark thin Ni_3P layer having large number of voids formed within the electroless Ni–P layer.

3.2. Aged reaction samples

Solid-state aging at 150 °C for 1000 h is a required reliability test for solder/UBM joint [4]. In this work, solid-state aging was carried out at higher temperatures (160 to 200 °C) to shorten the aging duration to 400 h. Fig. 4 shows the back-scattered SEM images of Sn–3.5Ag/Ni–P/Cu interfaces in the samples aged at 160 °C for 225 h showing the growth of Ni_3Sn_4 intermetallic and Ni_3P layer. It can be observed that in the sample with thin Ni–P, the electroless Ni–P layer completely transformed into Ni_3P, whereas in other samples, it was still present underneath the Ni_3P layer. The thickness of this completely transformed electroless Ni–P layer (~1.9 μm) is much smaller than that of as-plated electroless Ni–P layer (~3.9 μm). This shrinkage in the electroless Ni–P layer indicates that during the aging, Ni diffused out from the electroless Ni–P layer to form the Ni_3Sn_4, leaving behind a higher P content Ni–P (Ni_3P) layer within the electroless Ni– P layer. It can be observed that in all the samples, several voids formed in the Ni_3P layer due to the depletion of Ni. However, a layer of voids also formed at the Ni_3P/Cu interface in the sample with thin Ni–P (Fig. 4a). In addition, in this sample, the Ni_3Sn_4 intermetallic was found to have Cu up to 5 at.%. The presence of Cu in the Ni_3Sn_4 and formation of layer of voids at the Ni_3P/Cu interface imply that the Cu diffused out from the Cu substrate to the Ni_3Sn_4 in the samples with thin Ni–P.

Fig. 5 shows the back-scattered SEM images of Sn–3.5Ag/Ni–P/Cu interfaces in the samples aged at 180 °C for 225 h showing the growth of Ni_3Sn_4, Ni_3P, Ni–Sn–P, and Ni–Cu–Sn IFC layers. From Fig. 5, it is clear that the thickness of electroless Ni–P UBM influences the growth of IFCs. Along with the transformation of electroless Ni–P into Ni_3P, only Ni_3Sn_4 grew predominantly in the sample with thick Ni–P, whereas, Ni–Sn–P also grew in the other samples. This Ni–Sn–P layer grew at the expense of Ni_3P layer (Fig. 5a and b). The chemical composition of this Ni–Sn–P layer was found similar to that of Ni_2SnP compound. It can be seen that in the sample with thick Ni–P, the number of voids formed at the Ni_3P/Cu interface is negligible as compared to the other samples. In this sample, the Cu content of Ni_3Sn_4 intermetallic (<1 at.%) was also negligible as compared to the other samples having Cu up to 7 at.%.

Fig. 6 shows the back-scattered SEM images of Sn–3.5Ag/Ni–P/Cu interfaces in the samples aged at 200 °C for 400 h showing the growth of Ni–Cu–Sn, Ni–Sn–P, and Cu–Sn IFCs. It can be seen that electroless Ni–P layer completely dissolved into Ni–Sn–P in all the samples. In the sample with thin Ni–P, two layers of Cu–Sn intermetallics, Cu_6Sn_5 and Cu_3Sn, formed at the Ni–Sn–P/Cu interface. The Cu_3Sn formed close to Cu substrate, understood to be due to the large availability of Cu from the Cu substrate. In the sample with thin Ni–P, two Ni–Cu–Sn intermetallics of distinct colors, $(Ni_{1-x}Cu_x)_3Sn_4$ and $(Ni_{1-x}Cu_x)_6Sn_5$, also formed at the Ni_3Sn_4/Ni–Sn–P interface. On the other hand, no Cu–Sn or $(Ni_{1-x}Cu_x)_6Sn_5$ intermetallics were found to form in the samples with medium and thick Ni–P, however, $(Ni_{1-x}Cu_x)_3Sn_4$ formed with Cu up to 6 at.%.

4. Discussion

4.1. Growth mechanism of IFCs

In this study, it was found that various IFCs such as Ni_3Sn_4, Ni–Sn–P, Ni_3P, Cu–Sn, and Ni–Cu–Sn form during the Sn–3.5Ag/Ni–P/Cu interfacial reactions. Although formation of many of these IFCs has been reported in the several studies [2–12], understanding made on their growth mechanism is still not complete. From the present investigation, it is clear that during Sn–3.5Ag/Ni–P/Cu interfacial reactions, initially, Sn of solder reacts with electroless Ni–P to form Ni_3Sn_4 and Ni–Sn–P layer and then Ni_3Sn_4 intermetallic and Ni_3P compound grow on the different sides of Ni–Sn–P layer (Figs. 3 and 4). The dominant growth of Ni_3Sn_4, over that of Ni–Sn–P, suggests that Ni_3Sn_4 might have lower activation energy of formation than that of Ni–Sn–P.

For the growth of Ni_3Sn_4, Sn comes from the solder to the Ni_3Sn_4/Ni–Sn–P interface [5], where it reacts with Ni that is coming from the electroless Ni–P layer. The depletion of Ni from the electroless Ni–P layer causes its crystallization or transformation into Ni_3P compound [6]. During the crystallization, electroless Ni–P layer shrinks into columnar grains of Ni_3P. The shrinkage in electroless Ni–P layer, along the direction of growth of IFC layers, is compensated by the growth of Ni_3Sn_4 layer. Whilst in the perpendicular directions it is compensated by the counter flux of vacancies. These vacancies accumulate and form columnar Kirkendall voids in the Ni_3P layer.

The growth of Ni_3Sn_4, over that of Ni–Sn–P, is continued as long as Ni is available from the underlying electroless Ni–P layer; otherwise, Sn will react with Ni_3P layer to form Ni–Sn–P. The same was observed in the samples aged at 180 °C for 225 h and had thin and medium Ni–P layers, where electroless Ni–P layer completely transformed into Ni_3P (Fig. 5a and b). Subsequently, in the absence of Ni supply, Sn started reacting with Ni_3P layer to form Ni–Sn–P. After complete dissolution of Ni_3P layer into Ni–Sn–P, Sn reaches the Cu substrate and forms Cu_3Sn and Cu_6Sn_5 intermetallics at the Ni–Sn–P/Cu interface (Fig. 6a). At the same time, Cu starts diffusing out from the Cu surface to the Ni_3Sn_4/Ni–Sn–P interface and forms $(Ni_{1-x}Cu_x)_3Sn_4$ and $(Ni_{1-x}Cu_x)_6Sn_5$ intermetallics due to the reaction with Ni_3Sn_4. Initially, the $(Ni_{1-x}Cu_x)_3Sn_4$ intermetallic with low Cu content forms and then eventually the $(Ni_{1-x}Cu_x)_6Sn_5$ intermetallic with high Cu content (Table 1) forms due to the continued supply of Cu.

Since during the Sn–3.5Ag/Ni–P/Cu interfacial reactions, several IFCs such as Ni–Sn–P, Cu–Sn, and Ni–Cu–Sn grow only after complete crystallization of electroless Ni–P UBM. Thus, the growth of these IFCs can be hindered by preventing the complete crystallization of electroless Ni–P UBM and this can be achieved by increasing the Ni–P thickness.

4.2. Diffusion of Cu through Ni_3P layer

From the results, it can be observed that Cu diffuses through the Ni_3P layer (Figs. 4a and 5). However, the mechanism of Cu diffusion has to be understood. Electroless Ni–P UBM is a good diffusion barrier due to its amorphous structure. The amorphous structure lacks the grain boundaries and thus inhibits the grain boundary diffusion. The structure of electroless Ni–P generally depends upon its P content [13]; amorphous if P is higher than 12.5 at.% and nanocrystalline otherwise. Thus, the as-plated electroless Ni–P layer (with 16 at.% P) was amorphous in nature, which transformed into bi-layered Ni–P, crystalline Ni_3P layer on the electroless Ni–P layer, during the reflow (Fig. 3). This Ni_3P layer grew continuously at the expense of electroless Ni–P layer during the aging (Figs. 4 and 5). It was found previously [6,11] that the Ni_3P layer has columnar grains. Therefore, as this

layer reached the Cu substrate, Cu started diffusing through the grain boundaries of Ni_3P layer.

A schematic illustration of Cu diffusion through the Ni_3P layer is shown in Fig. 7. As Sn–3.5Ag/Ni–P interfacial reactions proceed, Ni diffuses out from the electroless Ni–P layer through the grain boundaries of Ni_3P layer to form Ni_3Sn_4 and thus results in the growth of Ni_3P layer (Fig. 7a). This process is continued until the Ni_3P layer reaches the Cu substrate; after that, Cu starts diffusing out from the Cu substrate through the grain boundaries of Ni_3P layer to compensate the Ni supply (Fig. 7b). It is to be understood that as long as electroless Ni–P layer is present on the Cu substrate, Cu cannot diffuse out due to the lack of grain boundaries in the electroless Ni–P. However, after its crystallization into Ni_3P, grain boundaries of Ni_3P layer provide diffusion paths for Cu atoms. Thus, the diffusion of Cu from the Cu substrate can be inhibited by preventing the complete crystallization of electroless Ni–P UBM, which directly depends upon the thickness of electroless Ni–P UBM.

5. Conclusions

In this study, solid-state interfacial reactions between Sn– 3.5Ag solder and electroless Ni–P UBM on Cu substrate were investigated for three different Ni–P thicknesses. The following conclusions were made based on the study

1. Initially, three distinct IFC layers, Ni_3Sn_4, Ni–Sn–P, and Ni_3P, form at the Sn–3.5Ag/Ni–P interface during the interfacial reactions. The Ni_3P layer grows within the electroless Ni–P layer due to the depletion of Ni. Columnar voids form in the Ni_3P layer to compensate the Ni depletion.
2. As the Ni_3P layer reaches the Cu substrate, Cu starts diffusing out from the Cu substrate through the grain boundaries of Ni_3P layer and forms Ni–Cu–Sn intermetallics due to the reaction with Ni_3Sn_4. In the absence of Ni supply, Sn starts reacting with Ni_3P layer to form Ni–Sn–P. After complete dissolution of Ni_3P layer into Ni–Sn–P, Sn reaches the Cu substrate and forms Cu–Sn intermetallics at the Ni–Sn–P/Cu interface.

3. Thickness of electroless Ni–P UBM influences the growth of IFCs at the Sn–3.5Ag/Ni–P/Cu interfaces due to the amount of Ni available from the electroless Ni–P. In the samples with thin (3.9 μm) Ni–P, various IFCs such as Ni–Sn–P, Cu_3Sn, Cu_6Sn_5, $(Ni_{1-x}Cu_x)_3Sn_4$, and $(Ni_{1-x}Cu_x)_6Sn_5$ grew at lower aging temperature and within shorter duration as compared to the samples with thicker (7.3 and 9.9 μm) Ni–P. Thus, the growth of these IFCs can be avoided by using the Ni–P UBM of proper thickness.

Acknowledgements

This work was supported by School of Materials Science and Engineering, NTU, and Institute of Microelectronics. Helpful discussion with Dr. Andriy M. Gusak is gratefully acknowledged.

References

[1] C.Y. Liu, C. Chen, A.K. Mal, K.N. Tu, J. Appl. Phys. 85 (1999) 3882.

[2] M.O. Alam, Y.C. Chan, K.N. Tu, J. Appl. Phys. 94 (2003) 4108.

[3] Z. Chen, M. He, A. Kumar, G.J. Qi, J. Electron. Mater., in press.

[4] K.N. Tu, K. Zeng, Mater. Sci. Eng., R Rep. 34 (2001) 1.

[5] C.Y. Lee, K.L. Lin, Thin Solid Films 249 (1994) 201.

[6] J.W. Jang, P.G. Kim, K.N. Tu, D.R. Frear, P. Thompson, J. Appl. Phys. 85 (1999) 8456.

[7] P.L. Liu, Z. Xu, J.K. Shang, Metall. Mater. Trans., A Phys. Metall. Mater. Sci. 31A (2000) 2857.

[8] H. Matsuki, H. Ibuka, H. Saka, Sci. Technol. Adv. Mater. 3 (2002) 261.

[9] Y.D. Jeon, A. Ostmann, H. Reichl, K.W. Paik, Electron. Compon. Technol. Conf. (IEEE) (2003) 1203.

[10] S.J. Wang, C.Y. Liu, Scr. Mater. 49 (2003) 813.

[11] M. He, Z. Chen, G. Qi, Acta Mater. 52 (2004) 2047.

[12] A. Kumar, M. He, Z. Chen, Surf. Coat. Technol. 198 (2005) 283.

[13] G.O. Mallory, J.B. Hajdu, Electroless Plating: Fundamental and Applications, American Electroplaters and Surface Finishes Society, Orlando, 1990.

List of Tables

List of Figures

IFCs	Ni	Cu	Sn	P
Ni–Sn–P	45±1.5	<2	29±1.5	24±1.5
$(Ni_{1-x}Cu_x)_3Sn_4$	33±1	8±1	59±1	–
$(Ni_{1-x}Cu_x)_6Sn_5$	25±1.5	29±2.5	46±1.5	–
Cu_6Sn_5	–	52±1.5	48±1.5	–
Cu_3Sn	–	73±1.5	27±1.5	–

Table 1

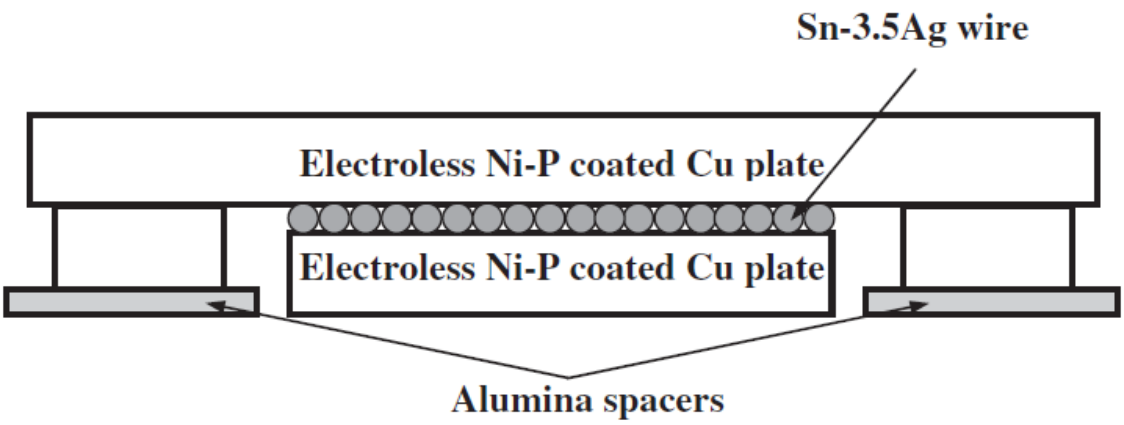
Sn-3.5Ag wire
Electroless Ni-P coated Cu plate
Electroless Ni-P coated Cu plate
Alumina spacers

Fig. 1

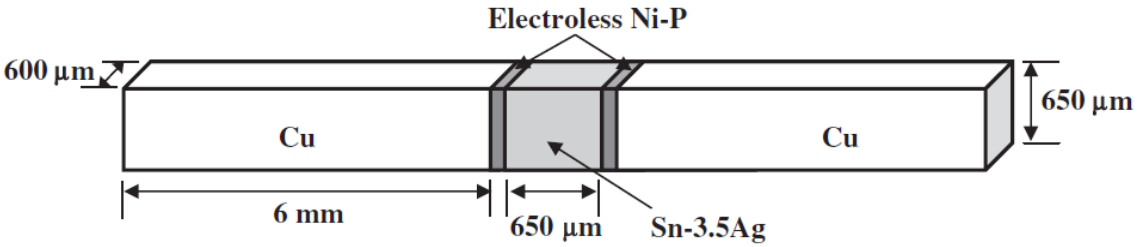

Fig. 2

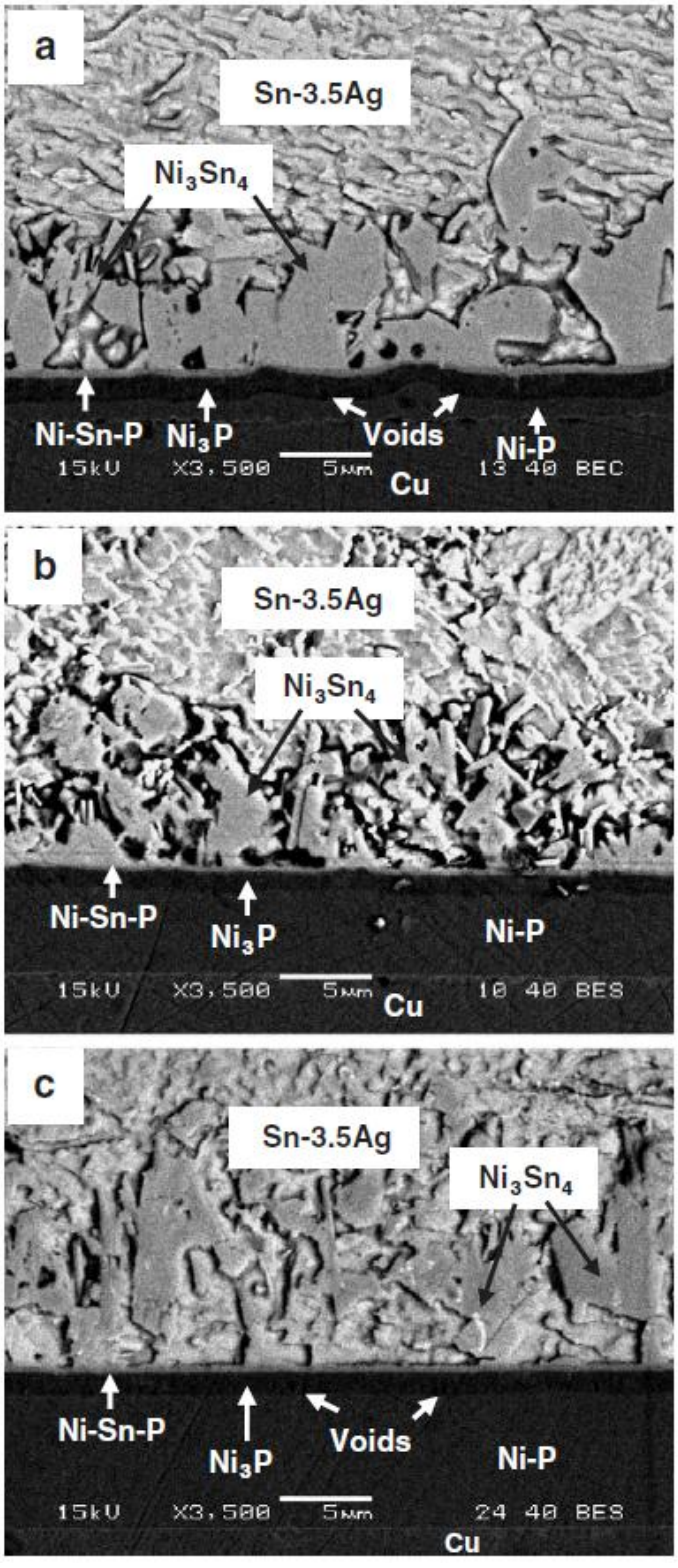
a
Sn-3.5Ag
Ni3Sn4
Ni-Sn-P
Ni3P
Voids
Ni-P
15kU X3,500 5µm
Cu
13 40 BEC
b
Sn-3.5Ag
Ni3Sn4
Ni-Sn-P
Ni3P
Ni-P
15kU X3,500 5µm
Cu
10 40 BES
c
Sn-3.5Ag
Ni3Sn4
Ni-Sn-P
Ni3P
Voids
Ni-P
15kU X3,500 5µm
24 40 BES
Cu

Fig. 3

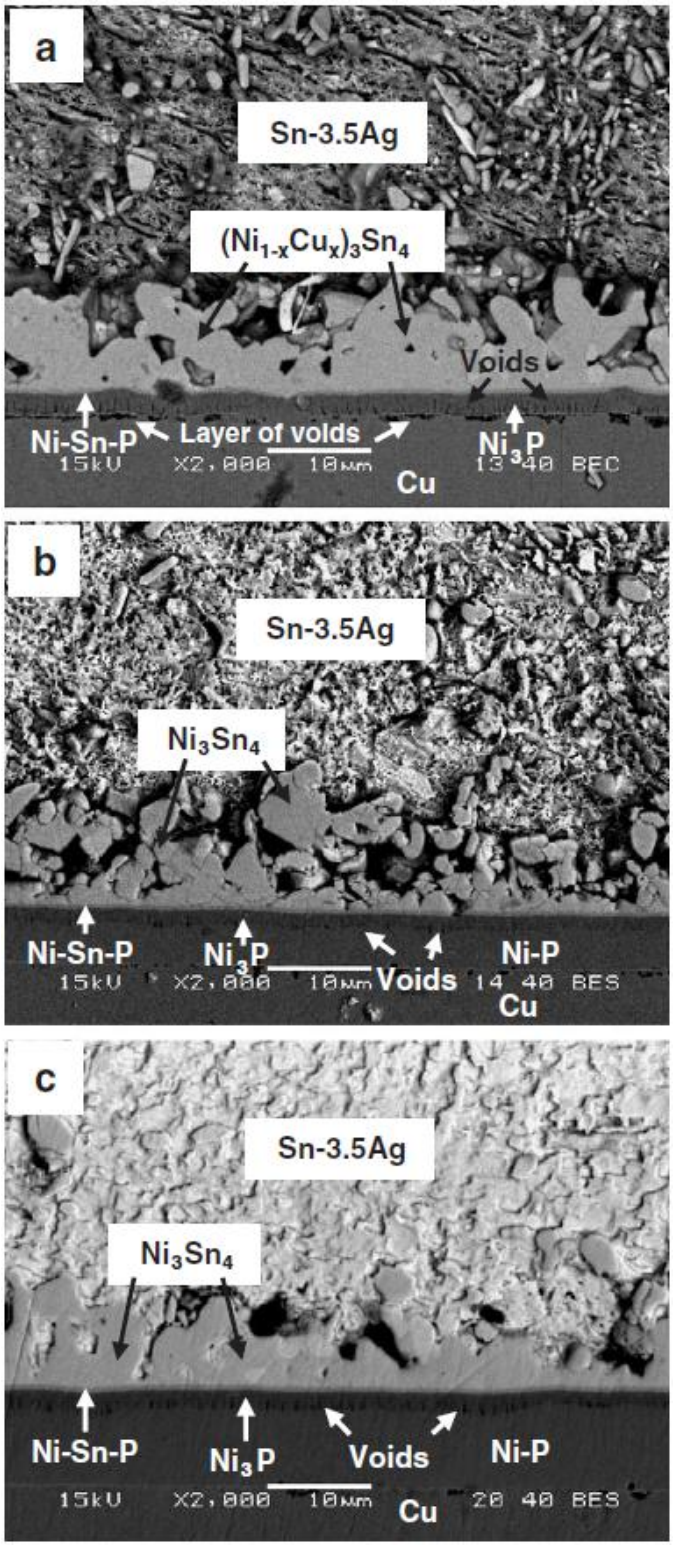
a
Sn-3.5Ag
$(Ni_{1-x}Cu_x)_3Sn_4$
Voids
Ni-Sn-P
Layer of voids
Ni_3P
15kV X2,000 10μm 13 40 BEC
Cu
b
Sn-3.5Ag
Ni_3Sn_4
Ni-Sn-P
Ni_3P
Voids
Ni-P
15kV X2,000 10μm 14 40 BES
Cu
c
Sn-3.5Ag
Ni_3Sn_4
Ni-Sn-P
Ni_3P
Voids
Ni-P
15kV X2,000 10μm 20 40 BES
Cu

Fig. 4

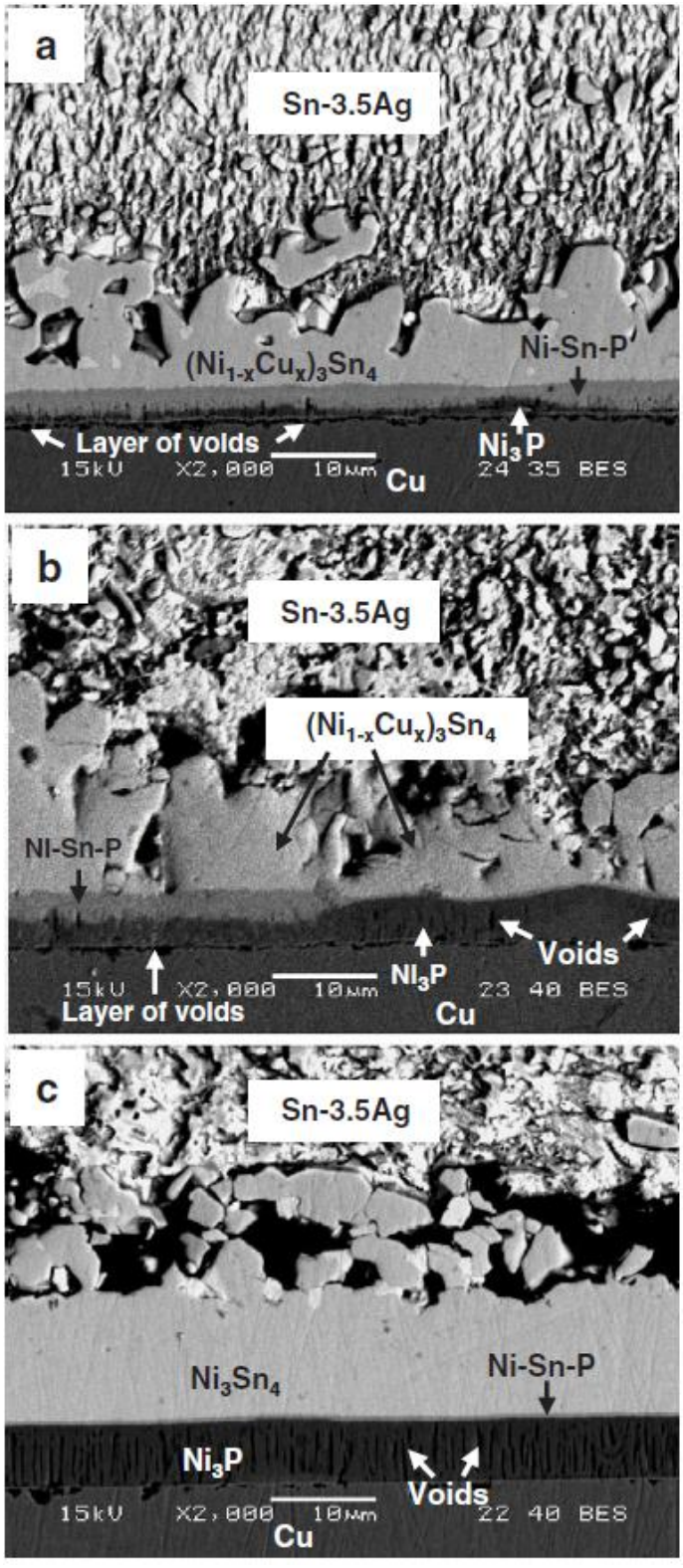
a
Sn-3.5Ag
$(Ni_{1-x}Cu_x)_3Sn_4$
Ni-Sn-P
Layer of volds
Ni_3P
15kV X2,000 10µm
Cu
24 35 BES
b
Sn-3.5Ag
$(Ni_{1-x}Cu_x)_3Sn_4$
NI-Sn-P
Voids
NI_3P
15kV X2,000 10µm
23 40 BES
Layer of volds
Cu
c
Sn-3.5Ag
Ni_3Sn_4
Ni-Sn-P
Ni_3P
Voids
15kV X2,000 10µm
22 40 BES
Cu

Fig. 6

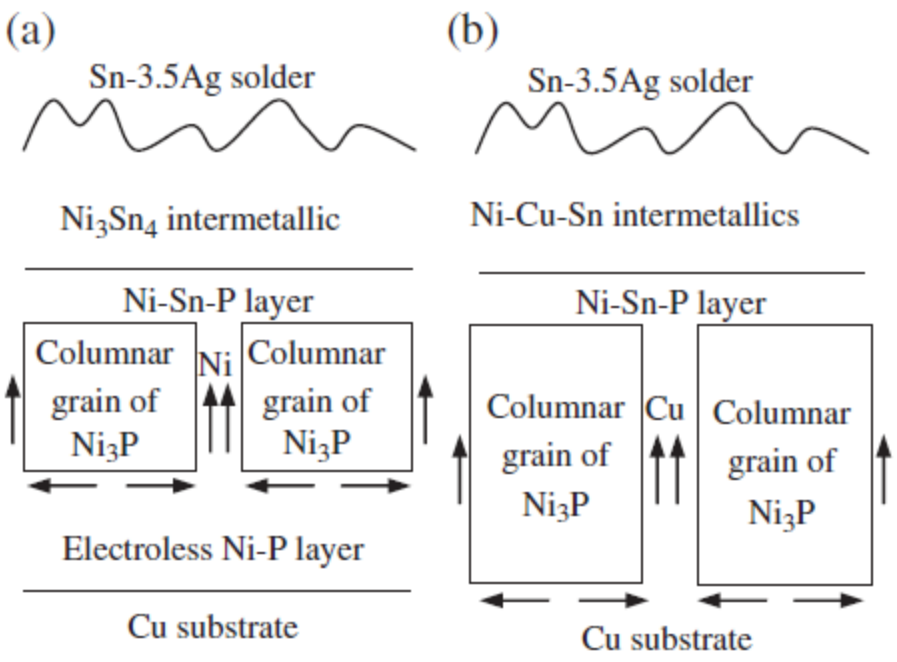
(a)
Sn-3.5Ag solder
Ni_3Sn_4 intermetallic
Ni-Sn-P layer
Columnar grain of Ni_3P
Ni
Columnar grain of Ni_3P
Electroless Ni-P layer
Cu substrate
(b)
Sn-3.5Ag solder
Ni-Cu-Sn intermetallics
Ni-Sn-P layer
Columnar grain of Ni_3P
Cu
Columnar grain of Ni_3P
Cu substrate

Fig. 7